Journal of Photochemistry and Photobiology A: Chemistry 210 (2010) 8–16

Contents lists available at ScienceDirect

Journal of Photochemistry and Photobiology A: Chemistry

journal homepage: www.elsevier.com/locate/jphotochem

Optical and photovoltaic properties of salicylaldimine-based azo ligands

Haluk Dinçalp[a,*], Sinem Yavuz[a], Özgül Haklı[b], Ceylan Zafer[c], Cihan Özsoy[c], İnci Durucasu[a], Sıddık İçli[c]

[a] Department of Chemistry, Faculty of Art and Science, Celal Bayar University, Muradiye, 45030 Manisa, Turkey
[b] Department of Chemistry, Faculty of Art and Science, Muğla University, Kötekli, 48000 Muğla, Turkey
[c] Solar Energy Institute, Ege University, Bornova, 35100 Izmir, Turkey

ARTICLE INFO

Article history:
Received 2 October 2009
Received in revised form 4 December 2009
Accepted 15 December 2009
Available online 23 December 2009

Keywords:
Azo dye
Solvatochromism
Photodecomposition
Complex formation
DSSC

ABSTRACT

A series of azo dyes containing salicylaldimine-based ligands as side chains were prepared and characterized. Absorption and emission data in five solvents of different polarities were studied. Photoirradiation studies under an oxygen atmosphere in water showed that the Schiff base side chains enhanced the photooxidative stability of the azo chromophore. The electrochemical properties of the dyes were investigated by a cyclic voltammetry. The synthesized salicylaldimine-based azo dyes gave two irreversible oxidation potentials. Complexation behavior of synthesized compounds with titanium (IV) ions was illustrated by the change in their absorption spectra. These ligands are appropriate sensitizers for anchoring to the TiO_2 surface chemically in dye-sensitized solar cell (DSSC) productions. Electron injection capacities to TiO_2 and photovoltaic performance of the synthesized salicylaldimine-based azo dyes were tested with DSSC.

1. Introduction

Azo dyes are well-known class of organic photoactive materials due to their excellent optical switching properties, good chemical stabilities and high solution process abilities [1,2]. These materials are widely used in heat transfer printing and textile industries [3,4], optical data storage [5], switching technologies [6] and photo-refractive polymer industries [7]. Also, azo dyes are used as sensitizers in dye-sensitized solar cells (DSSCs) based on photosensitization of nanocrystalline titanium dioxide (nc-TiO_2) [8]. Chelating activity with metal ions, easy and low cost production of azo dyes are some of their advantages with reference to other organic sensitizers used in DSSCs. In order to improve the photon-to-electric conversion efficiency (PCE), the dye has to be in close contact with the semiconductor surface. As a result, electron injection rate from the excited state HOMO level of the dye to the conduction band (CB) of metal oxides reaches to femto second level. In particular, the preferred dyes including anchoring groups such as carboxylates and phosphonates that provide an efficient interaction with the surface of semiconductor give a simple way to inject the electrons to the conduction band of the metal oxide [9].

Salicylaldimine-based azo ligands [10–13] are the most important class of chelating ligands that are extensively studied in coordination chemistry of transition metals. The Schiff bases form a series of complexes with most of the metal ions such as Cu(II) [14], Ni(II) and Zn(II) [15,16], Co(II) [16], Fe(III) [17]. Also, they are used as optical materials because of their interesting photochromic properties [18,19]. Schiff bases may become promising dye sensitizer in molecular photovoltaic cells if combined their chelating activities and other properties. In particular, the use of salicylaldimine-based azo ligands as sensitizers in DSSCs provides a direct interaction with the surface of TiO_2.

In the present work, we present three new azo dyes containing salicylaldimine group as sensitizers for DSSCs. The aim of attaching a nitro group at one end of the molecule is to obtain stable compound against oxidation. Nitro aromatic compounds are resistant to oxidative attack because of their electron-withdrawing nature [20]. We have synthesized the azo monomers combined with the salicylaldimine-based ligands substituted with different electron-withdrawing groups (Scheme 1). The characteristics of the absorption and emission spectra of the synthesized salicylaldimine-based azo ligands have been identified in five solvents of different polarities. Also, we have investigated the complexation behavior of the synthesized compounds with Ti(IV) ions. Photovoltaic performance of DSSCs based on these new type salicylaldimine compounds has been investigated.

2. Experimental details

2.1. Materials and methods

All reagents and solvents used were purchased from Merck Chemical Company. ^1H and ^{13}C NMR spectra were measured on a Bruker spectrometer operating at 400 MHz. The IR spectra of

* Corresponding author. Tel.: +90 236 2412151/2543; fax: +90 236 2412158.
E-mail address: haluk.dincalp@bayar.edu.tr (H. Dinçalp).

1010-6030/$ – see front matter © 2009 Elsevier B.V. All rights reserved.
doi:10.1016/j.jphotochem.2009.12.012

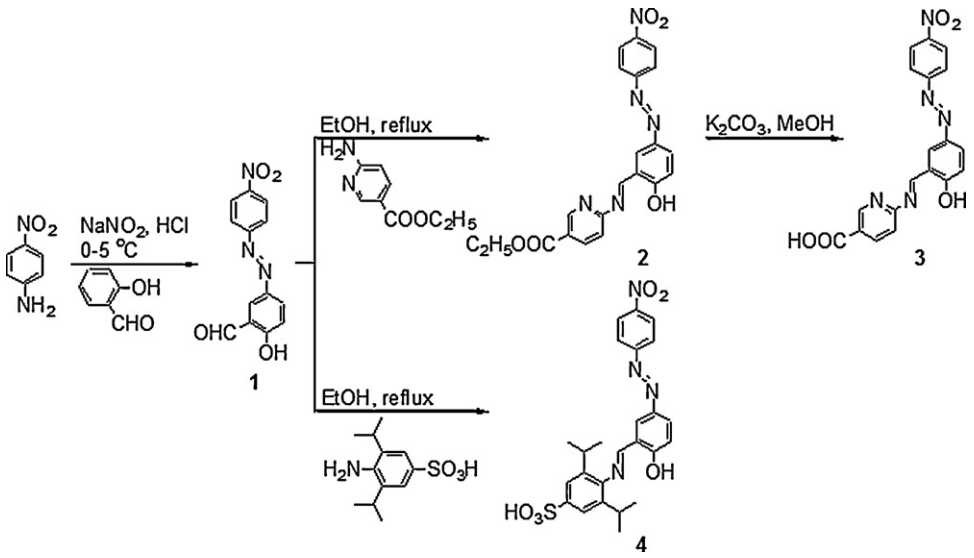

Scheme 1. Synthetic routes of azo dyes **1**–**4**.

the synthesized compounds were measured on a Perkin Elmer-Spectrum BX spectrophotometer by dispersing samples in KBr pellets. LC–MS spectroscopy was obtained on an Agilent 1100 MSD spectrometer.

UV–vis spectra measurements were performed by a JASCO V-530 UV–VIS diode array spectrophotometer, and fluorescence spectra measurements were performed with a PTI QM1 fluorescence spectrophotometer. Quantum yields of fluorescence were measured by comparing the fluorescence intensity of the sample to that of the optically dilute solutions of Riboflavin in ethanol (Φ_f = 0.30, λ_{exc} = 450 nm) [21]. All the experiments were carried out at 25 °C, and all the compounds were analyzed at an optical density of below 0.1.

Electrochemical properties of the materials were studied by cyclic voltammetry (CV). CV measurements were recorded by CH 660B model potentiostat from CH instruments using a three-electrode one-compartment cell equipped with a glassy carbon working electrode (WE), a platinum counter electrode (CE), and Ag/AgCl (in 3 M KCl solution) reference electrode (RE). The supporting electrolyte was 0.1 M [TBA][PF6] in acetonitrile. The milimolar solutions of the dyes were prepared in spectroscopic grade acetonitrile. The oxidation potential of ferrocene/ferrocenium redox couple (Fe/Fe^+) used as an internal reference was observed at +0.41 V.

2.2. Synthesis of TiO_2 nano-particles and electrode preparation

Synthesis of TiO_2 nano-particles was achieved by modification of procedure reported by Graetzel and co-workers [22]. 58.6 g titanium tetra isopropoxide $Ti(O^iPr)_4$ was added to 12 g glacial acetic acid. The solution was added dropwise into the 290 ml cooled deionized water under vigorous stirring, pH of the solution was adjusted to 1–2 by adding 5.4 ml nitric acid (65% HNO_3). The sol was peptized at 78 °C for 75 min in the oven, and then diluted to 370 ml by adding deionized water. The sol was transferred to the Teflon beaker equipped autoclave and heated at 235 °C for 12 h for hydrothermal growth of the particles. After cooling down the suspension, 2.4 ml nitric acid (65% HNO_3) was added and sonicated with ultrasonic horn 200 W power for 10 min in order to break agglomerates. Then, the suspension was concentrated to 16.5% (w/w) TiO_2. Remaining all water was exchanged with ethanol by centrifuging and 40% (w/w) TiO_2 paste was obtained. After the addition of 4.5% ethyl cellulose in ethanol and 79 g anhydrous α-terpineol, the obtained paste was sonicated again by ultrasonic horn at 200 W power for 10 min. All the ethanol in the paste was removed by rotary evaporator.

The TiO_2 paste was coated on transparent SnO_2 coated glass electrodes (SnO_2: F, TEC15, R_{sheet}: 15 ohm/□) by screen printing technique (polyester screen with 77 T mesh). Dried TiO_2 electrodes were sintered at 500 °C for 1 h with 10 °C/min heating rate. Finally, mesoporous TiO_2 film with 20 nm particle size and 4 μm thicknesses was obtained.

2.3. Sensitization with dye and DSSC assembly

TiO_2 electrodes were immersed in dye solution containing 0.3 mM **Z-907** in acetonitrile:*tert*-butanol (1:1), 0.3 mM azo dyes **3** and **4** in chloroform:methanol (1:1) overnight while electrode temperature is around 100 °C. Sensitized TiO_2 electrodes were rinsed with pure acetonitrile and kept in desiccator. Platinized FTO coated electrode was used as a counter electrode was prepared by thermal reduction of 1% (v/v) 2-propanol solution of hexachloroplatinic acid to the metallic platinum. Drop casted electrodes annealed at 380 °C for 30 min. The DSSCs were prepared by placing the electrodes in sandwich geometry top of each other and in the middle 50-μm thick thermoplastic polymer frame Surlyn® 1702 (DuPont). The electrodes sealed by heating around 100 °C and pressing slightly. Electrolytes consist of iodide/triiodide redox couple filed into cell via pre-drilled small hole by vacuum. The electrolyte composition was 0.6 M 1-butyl-3-methyl-imidazolium iodide (BMII), 0.1 M lithium iodide (LiI), 0.05 M iodine (I_2) dissolved in 3-methoxy propyonitrile (MPN). The active areas of the prepared solar cells adjusted to 1.0 cm^2 by using mask.

The performance of the dye-sensitized TiO_2 solar cells was compared to the commercially available ruthenium dye (**Z-907**) Ru(4,4′-dicarboxy-2,2′-bipyridine)(4,4′dinonyl-2,2′bipyridine)$(NCS)_2$. The photovoltaic characterizations of the DSSCs were done under the dark and standard conditions by illumination of AM1.5 global radiation with 100 mW/cm^2 light intensity.

The photovoltaic parameters of DSSC solar cells can be obtained from the following equations:

$$FF = \frac{V_m I_m}{V_{oc} I_{sc}} \quad (1)$$

and

$$\eta = \frac{I_{sc}V_{oc}FF}{P_{light}A} \quad (2)$$

where *FF* is filling factor, V_{oc} is the open circuit voltage, I_{sc} is the short current. I_m and V_m are the current and potential maximum power point, respectively, P_{light} is the intensity of incident light, and *A* is the cell area.

2.4. Synthesis

2.4.1. Synthesis of 6-aminoethyl nicotinate

A mixture of 2 g (14.5 mmol) of 6-aminonicotinic acid, 6.2 ml (106.5 mmol) of absolute ethanol and 2.7 ml of concentrated sulfuric acid on a steam bath was refluxed for 5 h. The solution was cooled to room temperature and slowly poured on to 12 g of crushed ice. A sufficient ammonia solution was added until the resulting solution was alkaline. The mixture was extracted with three 25 ml portions of ether. The combined ethereal extracts were dried over magnesium sulfate. Then, the ether was removed by flash distillation. The purity of the compound was controlled by TLC (chloroform:methanol/60:40). $C_8H_{10}O_2N_2$, Yield: 78%, FT-IR (KBr, cm^{-1}): 3411 and 3322 (ν_{N-H}), 3137, 1692 ($\nu_{C=O}$ ester), 1647, 1600, 1513, 1367, 1272, 1135 cm^{-1}. ^1H NMR (400 MHz, $CDCl_3$, δ 7.26 ppm): δ = 8.67 (1H, s); 8.02 (1H, dd, J_1 = 8.6 Hz, J_2 = 2.3 Hz); 6.51 (1H, d, J = 8.6 Hz); 5.41 (2H, broad s); 4.33 (2H, q, J = 7.0 Hz); 1.35 (3H, t, J = 7.0 Hz) ppm.

2.4.2. Synthesis of 3,5-diisopropyl-4-aminobenzenesulfonic acid

8.7 ml of concentrated sulfuric acid was added dropwise to the 10 ml (50 mmol) of 92% 2,6-diisopropyl aniline in an ice-bath with vigorous stirring. The mixture was stirred at 180 °C for 5 h. Then, the reaction mixture was cooled to room temperature and poured on to 80 g of crushed ice. The black precipitate was collected by a suction filtration. The precipitate was dissolved in 100 ml of boiling water and the solution was treated with 1 g of decolorizing charcoal. The mixture was stirred for 15 min and clarified by a suction filtration. The precipitate was collected by a suction filtration, washed well with cold water and recrystallized from water to give white crystals. $C_{12}H_{19}O_3NS$, Yield: 40%, FT-IR (KBr, cm^{-1}): 3400 (ν_{O-H}), 3126 and 3092 (ν_{N-H}), 2969 and 2873 (ν_{C-H} isopropyl), 1625, 1549, 1233, 1177, 1076, 1040, 735, 640 cm^{-1}. ^1H NMR [400 MHz, DMSO-d6, δ 2.48 ppm (5 peaks)]: δ = 7.41 (2H, s); 3.15 (2H, m, J = 7.0 Hz); 1.17 (12H, d, J = 7.0 Hz) ppm. ^{13}C NMR [100 MHz, DMSO-d6, δ 40.85 ppm (7 peaks)]: 146.64; 139.87; 129.53; 121.84; 27.74 (–**C**H(CH_3)$_2$); 24.00 (–CH(**C**H_3)$_2$) ppm.

2.4.3. Synthesis of 1-[3-(((4-ethylcarboxylate pyridyl)imino)methyl)-4-hydroxyphenylazo]-4-nitrobenzene (**2**)

The title compound was prepared using a procedure given in the patent application [23]. A mixture of 0.5 g (1.84 mmol) of azo dye **1** [26] and 0.31 g (1.84 mmol) of 6-aminoethyl nicotinate in 20 ml of ethanol was refluxed under a nitrogen atmosphere with stirring for 8 h. The reaction was monitored by TLC (toluene:methanol/90:10). The mixture was cooled to room temperature and an orange precipitate was filtered by a suction filtration. The solid was recrystallized from ethyl acetate to afford orange crystals. $C_{21}H_{17}O_5N_5$, Yield: 85%, FT-IR (KBr, cm^{-1}): 3316 (ν_{O-H}), 1709 ($\nu_{C=O}$ ester), 1622 ($\nu_{CH=N}$), 1588, 1558 and 1521 ($\nu_{N=N}$; *cis* and *trans*), 1342 (ν_{NO_2}), 1104, 1018 cm^{-1}. ^1H NMR (400 MHz, $CDCl_3$, δ 7.25 ppm): δ = 9.65 (1H, s); 9.15 (1H, s); 8.42 (1H, d, J = 1.6 Hz); 8.40 (2H, dd); 8.37 (1H, d); 8.24 (1H, d, J = 1.6 Hz); 8.14 (1H, dd, J_1 = 9.4 Hz, J_2 = 2.3 Hz); 8.02 (2H, d, J = 8.6 Hz); 7.40 (1H, d, J = 7.8 Hz); 7.17 (1H, d, J = 9.4 Hz); 4.45 (2H, q, J = 7.0 Hz); 1.44 (3H, t, J = 7.0 Hz) ppm. ^{13}C NMR [100 MHz, $CDCl_3$ δ 77 ppm (3 peaks)]: 110–166 (17 different C atoms including aromatic and imine C atoms); 61.76 (–O–**C**H_2–); 14.50 (–CH_2–**C**H_3) ppm. LC/MS–API-ES: $[M]^{\bullet+}$ = 419 molecular ion peak; 348 $[M]^{\bullet+}$–$COOC_2H_5$; 314 $[M]^{\bullet+}$–NO_2–OH–OC_2H_5; 286 $[M]^{\bullet+}$–NO_2–OH–$COOC_2H_5$; 270 $[M]^{\bullet+}$–$C_8H_8NO_2$; 256 $[M]^{\bullet+}$–$C_8H_8N_2O_2$; 167; 149; 113.

2.4.4. Synthesis of 1-[3-(((4-carboxypyridyl)imino)methyl)-4-hydroxyphenylazo]-4-nitrobenzene (**3**)

50 mg (0.12 mmol) of azo dye **2** was added to a solution of 16 mg (0.12 mmol) of potassium carbonate in 4 ml of methanol. The mixture was heated to boiling for 30 min or until no starting compound could be detected on TLC (toluene:methanol/90:10) plate. The reaction mixture was cooled to room temperature. A solution of the concentrated hydrochloric acid in methanol was added dropwise into the reaction mixture with vigorous stirring and the pH value of the solution was adjusted to 5. A red precipitate was collected by a suction filtration. The pure product was dried at 80 °C overnight. $C_{19}H_{13}O_5N_5$, Yield: 92%, FT-IR (KBr, cm^{-1}): 3434 (ν_{O-H}), 1717 ($\nu_{C=O}$ carboxylic acid), 1616 ($\nu_{CH=N}$), 1588, 1558, 1518 and 1474 ($\nu_{N=N}$; *cis* and *trans*), 1342 (ν_{NO_2}), 1286, 1104, 1004 cm^{-1}. ^1H NMR [400 MHz, DMSO-d6, δ 2.42 ppm (5 peaks) and 3.29 H shift of water]: δ = 10.35 (1H, s); 8.48 (1H, d, J = 2.3 Hz); 8.41 (2H, d, J = 9.4 Hz); 8.24 (1H, d, J = 2.3 Hz); 8.14 (1H, dd, J_1 = 8.6 Hz, J_2 = 2.3 Hz); 8.04 (2H, d, J = 8.6 Hz); 7.81 (1H, dd, J_1 = 8.6 Hz, J_2 = 2.3 Hz); 7.19 (1H, d, J = 9.4 Hz); 6.78 (1H, s); 6.44 (1H, d, J = 9.4 Hz) ppm. LC/MS–API-ES: $[M]^{\bullet+}$ = 391 molecular ion peak; 348 $[M]^{\bullet+}$–COOH; 314 $[M]^{\bullet+}$–NO_2–2OH; 286 $[M]^{\bullet+}$–NO_2–OH–COOH; 267; 258; 167; 149; 113.

2.4.5. Synthesis of 1-[3-(((2,6-diisopropyl-4-sulfophenyl)imino)methyl)-4-hydroxyphenylazo]-4-nitrobenzene (**4**)

A similar procedure to the one given above was followed. A mixture of 0.3 g (1.1 mmol) of azo dye **1** and 0.28 g (1.1 mmol) of 3,5-diisopropyl-4-aminobenzenesulfonic acid in 10 ml of ethanol was refluxed under a nitrogen atmosphere with stirring for 6 h. The mixture was cooled to room temperature and a pale red precipitate was filtered by a suction filtration. The purity of the compound was controlled by TLC (chloroform:methanol/90:10). $C_{25}H_{26}O_6N_4S$, Yield: 87%, FT-IR (KBr, cm^{-1}): 3434 (ν_{O-H}), 2969 (ν_{C-H} isopropyl), 1625 ($\nu_{CH=N}$), 1527 ($\nu_{N=N}$), 1342 (ν_{NO_2}), 1183, 1043 cm^{-1}. ^1H NMR [400 MHz, DMSO-d6, δ 2.47 ppm (5 peaks) and 3.29 H shift of water]: δ = 8.75 (1H, s); 8.44 (1H, d, J = 1.6 Hz); 8.41 (2H, d, J = 8.6 Hz); 8.10 (1H, dd, J_1 = 8.6 Hz, J_2 = 1.6 Hz); 8.04 (2H, d, J = 8.6 Hz); 7.45 (2H, s); 7.20 (1H, d, J = 8.6 Hz); 2.90 (2H, m, J = 7.0 Hz); 1.12 (12H, d, J = 7.0 Hz) ppm. ^{13}C NMR [100 MHz, DMSO-d6, δ 40.49 ppm (7 peaks)]: 119–166 (15 different C atoms including aromatic and imine C atoms); 28.47 (–**C**H(CH_3)$_2$); 23.85 (–CH(**C**H_3)$_2$) ppm. LC/MS–API-ES: $[M]^{\bullet+}$ = 510 molecular ion peak; 422 $[M]^{\bullet+}$–2CH(CH_3)$_2$; 391 $[M]^{\bullet+}$–$C_6H_4NO_2$; 348 $[M]^{\bullet+}$–2CH(CH_3)$_2$–SO_3H; 286 $[M]^{\bullet+}$–NO_2–OH–2CH(CH_3)$_2$–SO_3H; 267 $[M]^{\bullet+}$–$C_{12}H_{17}O_3S$; 258 $[M]^{\bullet+}$–$C_{12}H_{17}NO_3S$; 167; 149; 113.

3. Results and discussion

3.1. Spectral properties of dyes

Normalized steady-state absorption spectra of the reference compound azo dye **1** and salicylaldimine-based azo ligands in THF at room temperature are shown in Fig. 1. The reference compound azo dye **1** shows characteristic absorption peaks at 362 nm and a shoulder band at 457 nm, which are denoted to its (0,1) and (0,0) bands, respectively. Upon the introduction of salicylaldimine group to the azo benzene core, a bathochromic shift is observed.

We have studied the absorption and the fluorescence behaviors of azo dyes **1**–**4** in solvents of having different dielectric constants

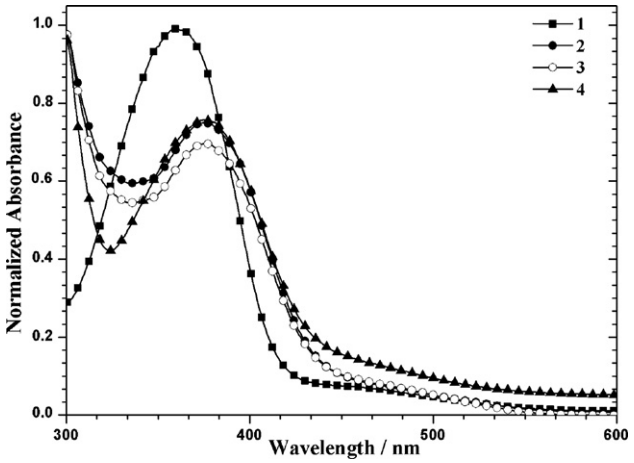

Fig. 1. Normalized UV–vis absorption spectra of azo dyes **1**–**4** in tetrahydrofuran.

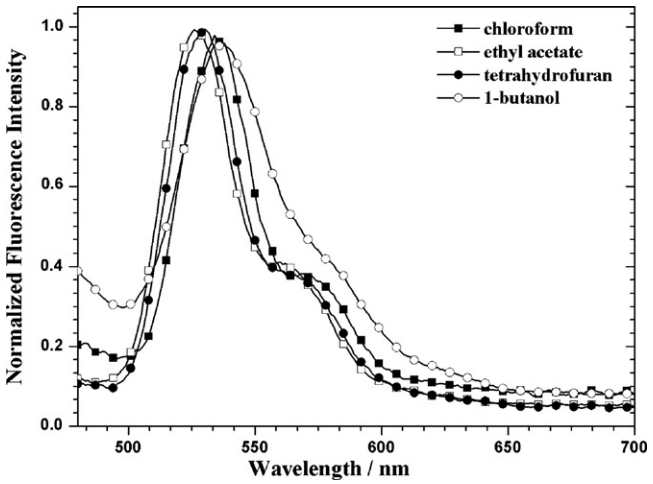

Fig. 2. Comparison of normalized fluorescence spectra of azo dye **3** in solvents of different polarities (λ_{exc} = 450 nm).

summarized in Table 1 and shown in Fig. 2. All of the compounds exhibit a major emission peak at a wavelength shorter than the minor peak. The major peak appears around 525 nm. The minor peak is seen as a red-shifted shoulder on the major emission peak. The emission spectra of all compounds in water (data not shown) are structureless while the same spectra give a good shape of bands in other organic solvents. The structurelessness of the emission bands in water solution may be attributed to the aggregation of azo dyes in water.

Another striking feature of the studied compounds is detected in the excitation spectra. It is well known that many salicylidene anilines exhibit inter- and intramolecular proton transfer reactions and give more than one structural form in the ground and excited states [24–27]. In our previous work, we demonstrated that the excited enol form of azo chromophores containing thiophene moiety and salicylaldimine-based ligand was converted to the keto form [28]. Also, it was noted that the hydrogen bonding ability of the solvents facilitated the formation of intramolecular hydrogen bonded enolic forms [29]. Fig. 3 gives a comparison of the UV–vis and the excitation spectra of azo dye **3** in ethyl acetate. Excitation spectrum of azo dye **3** at the collected emission wavelength of 530 nm is not identical with S_0–S_1 absorption band of the dye.

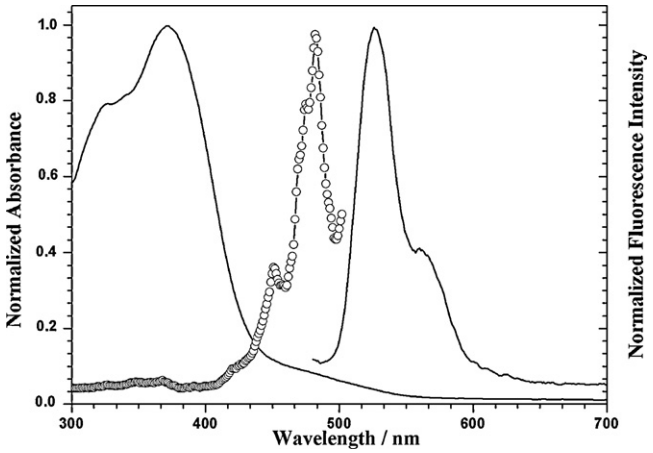

Fig. 3. Normalized UV–vis absorption, fluorescence and excitation spectra (with ball) of azo dye **3** in ethyl acetate (λ_{exc} = 450 nm, λ_{em} = 530 nm).

Table 1
The visible absorptions, fluorescence emissions, and Stokes shifts ($\Delta\lambda$) data of azo dyes **1**–**4** in solvents of different polarities (λ (nm), ε (l mol^{-1} cm^{-1})) (λ_{exc} = 450 nm).

Solvent	ε[a]	Compound	λ_{max}	ε_{max}	$\lambda_{max}^{longest}$	$\lambda_{em\,(max)}$	$\Delta\lambda$
Chloroform	4.8	**1**	359	20,900	466	529	79
		2	379	20,830	485	534	84
		3	378	17,270	485	534	84
		4	267	2660	457	528	78
Ethyl acetate	6.0	**1**	356	21,800	465	527	77
		2	373	21,270	482	526	76
		3	370	11,450	485	526	76
		4	277	3600	457	517	67
Tetrahydrofuran	7.6	**1**	362	20,180	468	528	78
		2	271	8610	484	528	78
		3	273	12,150	484	530	80
		4	268	6500	457	528	78
1-Butanol	17.8	**1**	380	16,830	461	525	75
		2	407	7520	451	536	86
		3	276	2990	454	536	86
		4	380	9940	467	528	78
Water	80.2	**1**	381	1140	457	533	83
		2	447	2010	447	530	80
		3	448	1960	448	529	79
		4	379	5670	453	529	79

[a] Dielectric constant, ε, is taken from Ref. [30].

Table 2
Fluorescence emission data, fluorescence quantum yields (Φ_f), radiative lifetimes (τ_0 (ns)), fluorescence lifetimes (τ_f (ns)), fluorescence rate constants ($k_f^r \times 10^8$ (s^{-1})), non-radiative rate constants ($k^{nr} \times 10^{11}$ (s^{-1})), and singlet energies (E_s (kcal mol^{-1})) of azo dyes **1**–**4** in solvents of different polarities (λ_{exc} = 450 nm)[a].

Solvent	Compound	Φ_f	τ_0	τ_f	k_f^r	k^{nr}	E_s
Chloroform	**1**	0.0011	1.9	0.002	5.2	4.9	62.2
	2	0.0025	1.6	0.004	6.1	2.5	59.8
	3	0.0016	1.6	0.003	6.3	3.8	59.8
	4	0.0012	4.9	0.006	2.1	1.7	63.4
Ethyl acetate	**1**	0.0049	1.7	0.009	5.7	1.1	62.4
	2	0.0012	1.6	0.002	6.4	5.3	60.2
	3	0.0023	2.4	0.006	4.1	1.8	59.8
	4	0.0011	5.6	0.006	1.8	1.6	63.4
Tetrahydrofuran	**1**	0.0012	1.5	0.002	6.6	5.6	62.0
	2	0.0013	2.2	0.003	4.6	3.7	60.0
	3	0.0024	1.5	0.004	6.7	2.8	59.9
	4	0.0017	2.9	0.005	3.4	1.9	63.4
1-Butanol	**1**	0.0007	2.0	0.001	5.1	7.5	63.0
	2	0.0013	7.0	0.009	1.4	1.1	64.3
	3	0.0018	6.1	0.011	1.7	0.9	63.8
	4	0.0008	3.6	0.003	2.8	3.3	62.1
Water	**1**	0.0016	1.4	0.002	7.3	4.4	63.5
	2	0.0008	0.4	<0.001	23.5	30.4	64.8
	3	0.0005	0.2	<0.001	55.3	101.0	64.7
	4	0.0005	3.3	0.002	3.1	6.6	64.0

[a] Photophysical parameters are calculated with the formulas: $\tau_0 = 3.5 \times 10^8$ ($\upsilon^2_{max}\, \varepsilon_{max}\, \Delta\upsilon_{1/2}$), $k_f = 1/\tau_f = k_f^r + k^{nr}$, $k_f^r = 1/\tau_0$, $\tau_f = \tau_0\, \Phi_f$ [31,32].

It shows a sharp peak at 480 nm and a minor peak at 450 nm. Additionally, the normalized emission spectra of the azo dye **3** have no mirror-image relationship with their respective absorption spectrum. These results support the intramolecular proton transfer reaction in the excited state and explain the formation of keto form of the compound. All of the excitation measurements of azo dyes **1**–**4** with the employed solvents have given similar results (data not shown). Although the reference compound azo dye **1** has no salicylaldimine group as side chains, *p*-hydroxyl group initiates the formation of hydrazone tautomer. However, in other structures, the most possible position of the tautomerization is between the hydroxyl group and the Schiff base group.

No clear relationship is determined between the solvent polarity and the absorption or emission wavelengths of the studied molecules, excluding those in 1-butanol and water solutions. The compounds give a marked bathochromic shift in absorption and emission maxima in these solutions compared to the same spectra recorded in chloroform, ethyl acetate, and tetrahydrofuran. Hydrogen bonding ability of the compounds with 1-butanol or water is evidently stronger than that of the solvents containing no hydroxyl moieties. Proton donating ability of the solvents stabilizes the charge transfer state better than the ground state of the molecule due to the interaction of the protons with the unshared electron pairs of the enol oxygen and the diazo nitrogen atoms and enhance the formation of inter- and intramolecular hydrogen bonded enolic form of the molecule, which creates a charge transfer acceptor form in the excited state. As a result, energy difference between the ground state and the excited state of the molecule decreases and a bathochromic shift occurs.

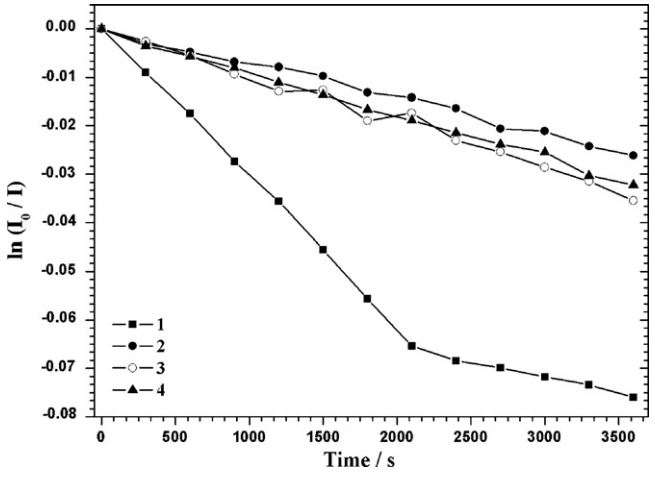

Fig. 4. Stern–Volmer plots of azo dyes **1**–**4** irradiated under Xe lamp exposure in the fluorescence spectrophotometer in water at the excitation wavelength of 450 nm for 1 h (λ_{em} = 530 nm) under an air oxygen atmosphere. Lineer equations: (**1**: $-2.2 \times 10^{-5}X - 0.0076$; R^2: 0.97), (**2**: $-7.2 \times 10^{-6}X - 3.8 \times 10^{-5}$; R^2: 1.0), (**3**: $-9.6 \times 10^{-6}X + 6.6 \times 10^{-5}$; R^2: 0.99) (**4**: $-8.8 \times 10^{-6}X - 3.7 \times 10^{-4}$; R^2: 1.0).

Aggregation tendency of the molecules in water is responsible for the lowest fluorescence quantum yield values among the studied solutions. Fluorescence quantum yields and calculated photophysical data of the compounds in solvents of different polarities are summarized in Table 2. High non-radiative decay rate constant values in water support the aggregation behaviors of the compounds in water solution. The longest radiative lifetimes are observed for azo dye **4**. Generally, fluorescence quantum yields of azo dye **4** in the studied solvents are lower than that of the other compounds. This behavior may be explained by the low tautomerization capability of the azo dye **4** in the respective solvents. Bulky isopropyl groups may prevent the replacement of hydrogen atom in the tautomerization process so that the less planar structural form of azo dye **4** is obtained. Conformational relaxation is increased with respect to the other studied compounds. As a result, fluorescence quantum yield of azo dye **4** decreases.

Table 3
Photodecomposition rate constants ($k_p \times 10^{-6}$ (s^{-1})) of azo dyes **1**–**4** obtained under Xe lamp exposure in the fluorescence spectrophotometer in water (λ_{exc} = 254 and 450 nm) for 1 h at the collected emission wavelength of 530 nm under an argon or an air oxygen atmosphere.

Dye	Saturated with argon		Saturated with air oxygen	
	254 nm	450 nm	254 nm	450 nm
1	21.2	3.5	34.8	22.1
2	44.5	2.8	4.7	7.2
3	18.7	1.8	52.1	9.6
4	22.9	34.0	11.5	8.8

Table 4
Cyclic voltammetry data for azo dyes **1**–**4**[a].

Dye	$E^0_{red\,3}$ (V)	$E^0_{red\,2}$ (V)	$E^0_{red\,1}$ (V)	$E^0_{ox\,1}$ (V)	$E^0_{ox\,2}$ (V)	LUMO-1 (eV)	LUMO (eV)	HOMO (eV)	HOMO-1 (eV)	E_{gap1} (eV)	E_{gap} (eV)
1	−1.33	−1.00	−0.72	1.18			−3.67	−5.57			1.90
2	−1.33	−0.98	−0.81	1.18	1.48	−3.41	−3.58	−5.57	−5.87	2.46	1.99
3	−1.40	−0.98	−0.81	1.18	1.48	−3.41	−3.58	−5.57	−5.87	2.46	1.99
4	−1.25	−1.00	−0.79	0.98	1.38	−3.39	−3.60	−5.37	−5.77	2.38	1.77

[a] $E_{LUMO} = -(4.8 + E^{onset}_{red})$, $E_{HOMO} = E_{LUMO} - E_{gap}$ [35].

3.2. Photostability of dyes

The dyes were irradiated by Xe lamp exposure in the fluorescence spectrophotometer in water for 1 h at the excitation wavelengths of 254 and 450 nm under argon or air atmosphere. Photodecomposition behaviors of the compounds have been detected by monitoring the decrease of the emission intensity at the collected emission wavelength of 530 nm (Fig. 4). Photodecomposition rate constants of azo dyes **1**–**4** are calculated by the formula [33], $\ln(I_0/I) = k_p \times t$, where I_0 and I are the emission intensities of the dyes before and after the irradiation, respectively, k_p is the photodegradation rate constant and t is the irradiation time. The results were summarized in Table 3. Photodecomposition rate constants at 254 nm are much higher than that of at 450 nm. Higher energy radiation at 254 nm initiates numerous radicalic reactions which accelerate the decomposition of molecule. As seen, it is obvious that molecular oxygen or excited oxygen species play a major role in the photo-fading of the azo dyes in aerated water solutions. Self-sensitized photo-oxygenation of azo dyes has attracted a considerable attention in the photodegradation of azo dyes even if their quantum yields of singlet oxygen are very low (10^{-3}) [34]. While azo dye **1**, which does not contain imine bond, shows a higher photodecomposition rate constant under illumination in the presence of oxygen, azo dye **2** is the most resistant molecule to photo-oxidative degradation among the studied compounds. Interaction of excited state of azo molecule with the singlet oxygen is a crucial point in the clarification of photo-fading pathway.

3.3. Electrochemical measurements

CV has been applied to investigate the redox behaviors of azo dyes **1**–**4** and to find out HOMO/LUMO energy levels. Fig. 5a and b shows cyclic voltammograms of the two studied compounds, azo dyes **2** and **4** in three-electrode cell. Each compound exhibits three reduction waves. The second reduction wave shows reversible behavior, and the others are irreversible. While two irreversible oxidation peaks are observed for azo dyes **2**, **3**, and **4**, only one irreversible oxidation peak is detected for azo dye **1**. Cyclic voltammetry data including HOMO and LUMO energy levels of the compounds are also summarized in Table 4. Electron-releasing capacity estimated from the HOMO/LUMO energy levels decreases as follows: **4** > **3** ≈ **2** > **1**. Azo dye **4**, having the highest values of HOMO energy level, exhibits the lowest oxidation state among the studied compounds. This is attributed to the presence of isopropyl group that is donating its electrons to the molecule via sigma bond. Better stability exhibition of azo dyes **2** and **3** is because of the presence of the carboxylate groups that gain an extra conjugation to the molecule.

3.4. Complex formation with titanium (IV) ions

Azo compounds and Schiff bases can bind to the nano-particles of most of the metal atoms upon complex formation or charge transfer complex via electron transfer from the dye molecule to the metal surface. A number of Ti(IV) complexes with bi-, tri- and tetra-dentate salen-type ligands in which the different amino units are incorporated into the ligand backbone have been shown in the literature [36–39].

The FT-IR spectrum recorded for the dye **3**-adsorbed TiO_2 surface gives a clear observation of interaction of dye structure with TiO_2 surface (Fig. 6a). The Schiff base CH=N vibration band at 1616 cm^{-1}, the azo group N=N isomers vibration bands at 1474 and 1518 cm^{-1} and carboxylic acid C=O vibration band at 1717 cm^{-1} of dye **3** on FT-IR spectra disappear, but new bands appear on the graph. An intense band at 2137 cm^{-1} is assigned to N–N stretching frequencies of dye **3**–Ti complex. It assumes that dinitrogen species have been greatly modified by coordination onto titanium. There is a rare example of a coordination process of Ti with azo dyes in the literature [40–42]. Also, FT-IR bands at 1706 and 1836 cm^{-1} are attributed to the stretching vibrations of the Schiff base CH=N group and the carboxylic acid C=O group of the complex structure. Also, iminium N–H infrared band of complex is observed at 3327

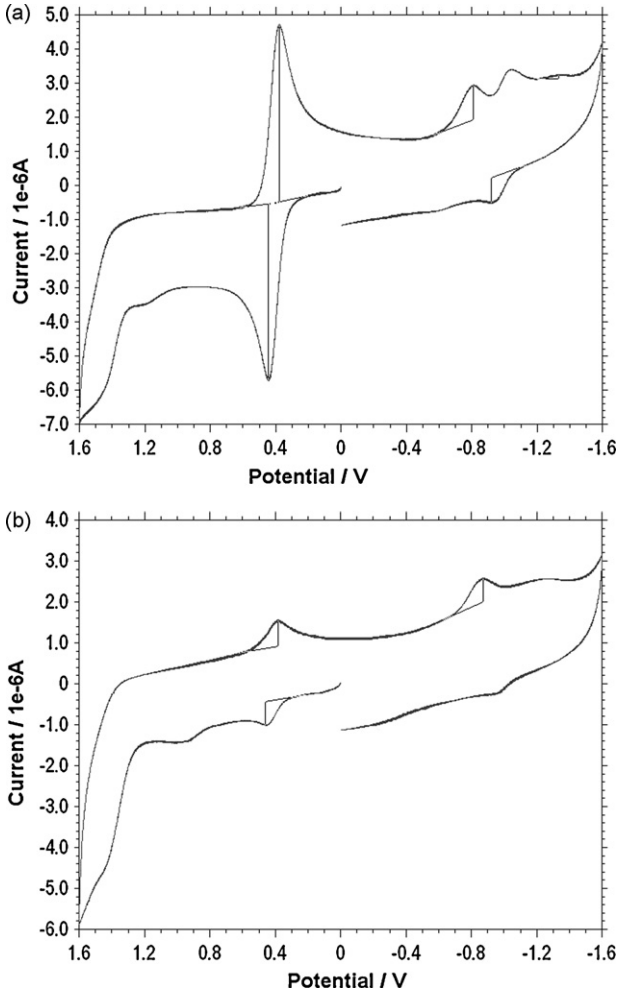

Fig. 5. Cyclic voltammograms at a glassy carbon electrode of (a) azo dye **2** (1 mM), and (b) azo dye **4** (1 mM) in MeCN containing 100 mM [TBA][PF6] and ferrocene as an internal electrode (E_{ox} = 0.41 V).

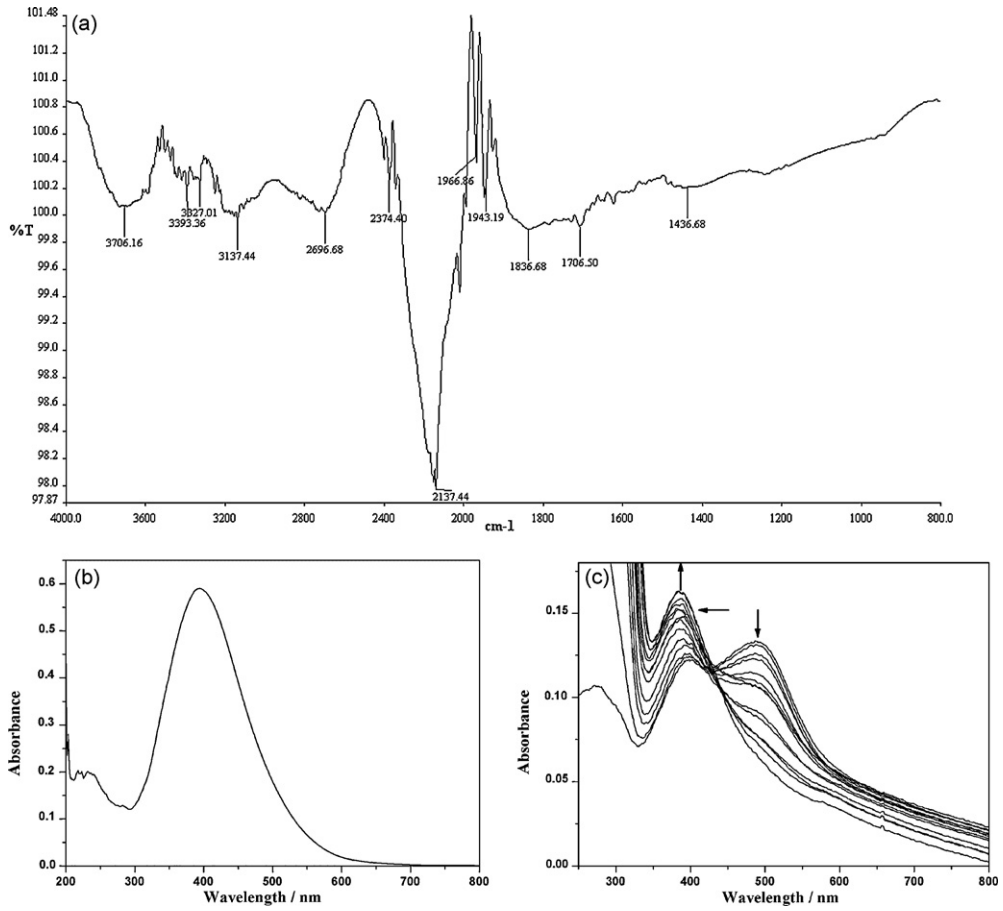

Fig. 6. (a) FT-IR/ATR and (b) UV–vis absorption spectrum of dye **3** adsorbed on TiO_2 surface. (c) Spectrophotometric titrations of dye **3** (4×10^{-5} M) with the addition of $Ti(O^iPr)_4$ in isopropanol. Changes in the absorbance with the addition of Ti^{4+} were illustrated by the arrows. [Ti^{4+}] (From down to up) = 0 M, 1.8×10^{-3} M, 3.7×10^{-3} M, 5.5×10^{-3} M, 7.3×10^{-3} M, 9.1×10^{-3} M, 10.9×10^{-3} M, 12.6×10^{-3} M, 14.4×10^{-3} M, 16.1×10^{-3} M, 17.8×10^{-3} M, 19.5×10^{-3} M, 21.2×10^{-3} M and 22.9×10^{-3} M.

and 3393 cm^{-1} as weak bands. UV–vis absorption spectrum of dye **3**-adsorbed TiO_2 surface is displayed in Fig. 6b. It shows a maximum at 394 nm corresponding to the electronic transition of the complex structure formed between TiO_2 particles and the dye structure.

In our study, at each addition 15 μl of titanium tetra isopropoxide $Ti(O^iPr)_4$ solution prepared in isopropanol at the concentration of 0.375 M was poured into the 3 ml isopropanol solution of 4×10^{-5} M compound **3**. The considerable amount of shift was observed in the absorption spectrum of dye molecule. Hypsochromic shift was observed from 399 to 385 nm for azo dye **3**. Also, absorption band at 490 nm disappears upon adding the Ti(IV) solution (Fig. 6c). This is attributed to the electronic interaction between the Ti(IV) ions and non-bonding electrons of oxygen or nitrogen atoms of salicylaldimine group. No obvious shift was observed for dye **4**–Ti complex formation. Also, bathochromic shifts were observed from 379 to 399 nm and 367 to 402 nm for azo dyes **2** and **1**, respectively (data not shown).

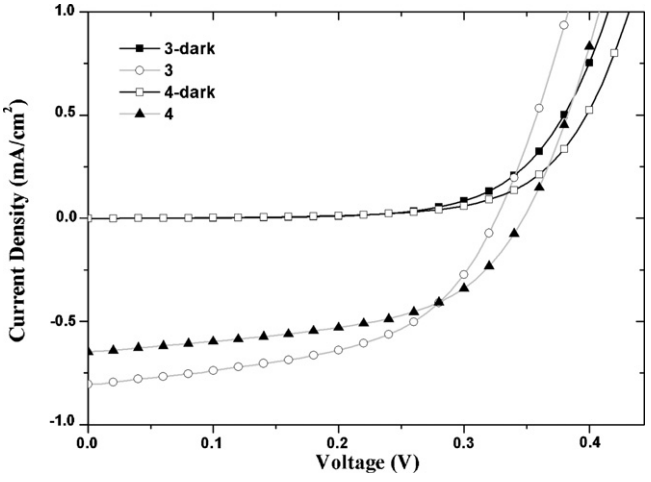

Fig. 7. Current–voltage graphs of azo dyes **3**–**4** in dark and under illumination with 100 mW/cm^2 light intensity.

3.5. Photovoltaic properties

Current–voltage (*I*–*V*) characteristics of the solar cells fabricated using azo dyes **3**–**4** were determined at standard conditions under illumination with simulated sunlight (AM1.5, 100 mW/cm^2 light intensity). Fig. 7 reveals the current density–voltage (*J*–*V*) charac-

Table 5
Photovoltaic parameters of DSSCs containing nc-TiO_2/azo dyes **3**–**4** photoactive electrodes, and standard dye **Z-907** under illumination with 100 mW/cm^2 light intensity.

Dye	Azo dye **3**	Azo dye **4**	**Z-907**
V_{oc} [V]	0.33	0.35	0.60
I_{sc} [mA/cm^2]	0.80	0.65	12.66
V_{mpp} [V]	0.24	0.26	0.38
I_{mpp} [mA/cm^2]	0.56	0.45	9.33
MPP [mW/cm^2]	0.14	0.12	3.55
FF	0.51	0.52	0.47
η [%]	0.14	0.12	3.55

Table 6
Advantages vs. disadvantages of dye **3** and **4** relative to one another.

Characteristics	Azo dye **3**	Azo dye **4**
FT-IR (cm^{-1})	1616 (m, $\nu_{CH=N}$)	1625 (s, $\nu_{CH=N}$)
Vis absorption[a] (nm)	490	375
Emission[b] (nm)	526–536	517–528
Fluorescence quantum yield[b]	0.0016–0.0024	0.0008–0.0017
Photodecomposition rate constant[c] (s^{-1})	9.6×10^{-6}	8.8×10^{-6}
Complex formation with Ti (IV)[a]	+14 (hypsochromic shift)	+4 (bathochromic shift)
HOMO (eV)	−5.57	−5.37
Band gap energy (eV)	1.99	1.77

[a] In isopropanol.
[b] In the studied solvents (chloroform, ethyl acetate, tetrahydrofuran, 1-butanol), λ_{exc} = 450 nm.
[c] In water, λ_{exc} = 450 nm, under O_2 atmosphere.

teristic of the photovoltaic devices. Photovoltaic performance data of the dyes are also given in Table 5. Open circuit voltage (V_{oc}) and short circuit photocurrent density (I_{sc}) for azo dye **3** are 0.33 V and 0.80 mA/cm^2, respectively, and those for azo dye **4** are 0.35 V and 0.65 mA/cm^2. These data implies much better performance of azo dye **3** with an overall conversion efficiency of 0.14% under illumination. The DSSC with azo dye **4** gives 0.52 fill factor yielding 0.12% efficiency. Several commercial mono and bis-azo dyes were studied as sensitizers in DSSCs containing TiO_2 photoanode and yielded good performance with V_{oc}. Especially, studied azo dyes containing salicylate chelating group were more strongly anchored to TiO_2 surface and produced higher short circuit photocurrent greater than 0.2 mA [43]. According to literature studies related to adsorption of azo dyes to TiO_2 surface, it is reported that some phenyl azo dyes functionalized with carboxyl and hydroxyl group were easily adsorbed on TiO_2 and ZnO electrodes and gave a strongly colored electrodes [44]. Selected azo dyes containing salicylate groups were also been used as sensitizers in Graetzel-type solar cells by El Mekkawi and Abdel-Mottaleb [45]. Salicylate groups facilitate the direct interaction of the dyes with TiO_2 surface, thereby convenient route to electron transfer from the LUMO level of dye to the conduction band of semiconductor occurred.

Investigated molecules, azo dyes **3** and **4**, strongly anchored on TiO_2 surface. Immersing TiO_2 electrodes in dye solution were coloured rapidly because of an effective interaction between the semiconductor surface and the dye structure. We observed faster decolorization of azo dye **3** solution during the DSSC assembly process. This is attributed to the chemical interaction between the TiO_2 surface and carboxylate group of the dye. Also, complex formation and charge transfer interaction between the nc-TiO_2 particles and salicylaldimine group of azo dyes **3** and **4** accelarates the electron injection from the excited state of the dye to the conduction band of semiconductor metal oxide. Photovoltaic cell with azo dye **3** shows better photovoltaic response as compared to the photovoltaic cell with azo dye **4**. This is attributed to the more effective electron injection from the LUMO level of azo dye **3** to the conduction band of TiO_2 through carboxylate bridge. Low chelating activity of azo dye **4** because of bulky isopropyl group causes a weak interaction between the dye and TiO_2 surface. This binding effect may reduce the electron transport possibility. Important issue to improve efficiency of the DSSC is to use a sensitizer based on donor-linker-acceptor molecular model.

Comparison of dyes **3** and **4** according to their advantages and disadvantages was summarized in Table 6. The LUMO energy levels of dyes **3** and **4** are higher than the conduction band of TiO_2. Therefore, these dyes are energetically suitable for TiO_2 based DSSCs. One of the advantages of dye **3** is lower HOMO energy level with respect to dye **4** resulting the lower charge recombination rate and higher driving force for dye regeneration. An important factor that produces low yield of efficiency for both of the dyes is the photodegradation pathway of the dyes in the presence of reactive oxygene species generated by TiO_2 catalyst under illumination. In addition, self-sensitized photooxidation of the azo dyes is crucial point in understanding the photodegradation pathways. Dyes show much higher photodecomposition rate constants in the presence of oxygen than that of a non-oxygenated atmosphere because of the formation of oxidation products resulted from self-sensitized photooxidation of azo dyes **1**–**4**. The tautomerization behavior and the steric factor play a role in the formation of charge transfer complex between the singlet oxygen and azo dyes **2**–**4**.

4. Conclusion

We have synthesized new water-soluble azo ligands containing a salicylaldimine group as a side chain to fabricate the DSSC. Also, we have studied the optical and electrochemical properties of the dyes to evaluate the photovoltaic performances. Steady-state spectroscopic measurements were carried out in solvents with increasing polarities. Aggregation tendency of the molecules in water was responsible for an unusual form of the steady-state measurements.

Chelating possibilities and steric factors change the favorable interaction of dyes with TiO_2 surface which affects overall photon-to-electric conversion efficiency (PCE) of DSSC. These preliminary studies show that salicylaldimine-based azo ligands are appropriate sensitizers for coordinating with TiO_2 surface in DSSC applications. New molecular modeling of azo dyes, which consist of donor-linker-acceptor moieties, is necessary to improve DSSC efficiency.

Acknowledgements

This project was supported by the Research Council of Celal Bayar University, the State Planning Organization of Turkey (DPT), the Research Center of Ege University, and Alexander von Humboldt Foundation of Germany.

References

[1] A. Vig, K. Sirbiladze, H.J. Nagy, P. Aranyosi, I. Rusznák, P. Sallay, The light stability of azo dyes and dyeings V. The impact of the atmosphere on the light stability of dyeings with heterobifunctional reactive azo dyes, Dyes Pigments 71 (2006) 199–205.
[2] M.M.M. Raposo, A.M.R.C. Sousa, A.M.C. Fonseca, G. Kirsch, Thienylpyrrole azo dyes: synthesis, solvatochromic and electrochemical properties, Tetrahedron 61 (2005) 8249–8256.
[3] A.T. Slark, P.M. Hadgett, The effect of specific interactions on dye transport in polymers above the glass transition, Polymer 40 (1999) 4001–4011.
[4] G. Hallas, J.H. Choi, Synthesis and properties of novel aziridinyl azo dyes from 2-aminothiophenes. Part 2. Application of some disperse dyes to polyester fibres, Dyes Pigments 40 (1999) 119–129.
[5] M.S. Ho, A. Natansohn, P. Rochon, Azo polymers for reversible optical storage. 7. The effect of the size of the photochromic groups, Macromolecules 28 (1995) 6124–6127.
[6] Y. Nabeshima, A. Shishido, A. Kanazawa, T. Shiono, T. Ikeda, T. Hiyama, Synthesis of novel liquid-crystalline thiophene derivatives and evaluation of their photoresponsive behavior, Chem. Mater. 9 (1997) 1480–1487.
[7] G. Iftime, F.L. Labarthet, A. Natansohn, P. Rochon, K. Murti, Main chain-containing azo-tetraphenyldiaminobiphenyl photorefractive polymers, Chem. Mater. 14 (2002) 168–174.
[8] G.D. Sharma, P. Suresh, S.K. Sharma, M.S. Roy, Photovoltaic properties of liquid-state photoelectrochemical cells based on PPAT and a composite film of PPAT and nanocrystalline titanium dioxide, Synth. Met. 158 (2008) 509–515.
[9] N. Robertson, Optimizing dyes for dye-sensitized solar cells, Angew. Chem. Int. Ed. 45 (2006) 2338–2345.
[10] K. Nejati, Z. Rezvani, B. Massoumi, Syntheses and investigation of thermal properties of copper complexes with azo-containing Schiff-base dyes, Dyes Pigments 75 (2007) 653–657.

[11] Z. Rezvani, B. Divband, A.R. Abbasi, K. Nejati, Liquid crystalline properties of copper(II) complexes derived from azo-containing salicylaldimine ligands, Polyhedron 25 (2006) 1915–1920.
[12] A.A. Khandar, Z. Rezvani, Preparation and thermal properties of the bis[5-((4-heptyloxyphenyl)azo)-N-(4-alkoxyphenyl)-salicylaldiminato]copper II complex homologues, Polyhedron 18 (1999) 129–133.
[13] A.A. Khandar, K. Nejati, Synthesis and characterization of a series of copper(II) complexes with azo-linked salicylaldimine Schiff base ligands. Crystal structure of Cu_5PHAZOSALTN·$CHCl_3$, Polyhedron 19 (2000) 607–613.
[14] E. Tas, A. Kilic, N. Konak, I. Yilmaz, The sterically hindered salicylaldimine ligands with their copper(II) metal complexes: synthesis, spectroscopy, electrochemical and thin-layer spectroelectrochemical features, Polyhedron 27 (2008) 1024–1032.
[15] V.P Daniel, B. Murukan, B.S. Kumari, K. Mohanan, Synthesis, spectroscopic characterization, electrochemical behaviour, reactivity and antibacterial activity of some transition metal complexes with 2-(N-salicylideneamino)-3-carboxyethyl-4,5-dimethylthiophene, Spectrochim. Acta Part A 70 (2008) 403–410.
[16] M.S. Nair, R.S. Joseyphus, Synthesis and characterization of Co(II), Ni(II), Cu(II) and Zn(II) complexes of tridentate Schiff base derived from vanillin and DL-α-aminobutyric acid, Spectrochim. Acta Part A 70 (2008) 749–753.
[17] E. Keskioğlu, A.B. Gündüzalp, S. Çete, F. Hamurcu, B. Erk, Cr(III), Fe(III) and Co(III) complexes of tetradentate (ONNO) Schiff base ligands: synthesis, characterization, properties and biological activity, Spectrochim. Acta Part A 70 (2008) 634–640.
[18] M.J. Baena, J. Barbed, P. Espinet, J.A. Ezcurra, M.B. Res, J.L. Serrano, Ferroelectric behavior in metal-containing liquid crystals: a structure–activity study, J. Am. Chem. Soc. 116 (1994) 1899–1906.
[19] N. Hoshino, H. Murakami, Y. Matsunaga, T. Inabe, Y. Maruyama, Liquid crystalline copper(II) complexes of N-salicylideneaniline derivatives. Mesomorphic properties and a crystal structure, Inorg. Chem. 29 (1990) 1177–1181.
[20] R. Friemann, M.M. Ivkovic-Jensen, D.J. Lessner, C.L. Yu, D.T. Gibson, R.E. Parales, H. Eklund, S. Ramaswamy, Structural insight into the dioxygenation of nitroarene compounds: the crystal structure of nitrobenzene dioxygenase, J. Mol. Biol. 348 (2005) 1139–1151.
[21] H. Du, R.C.A. Fuh, J.Z. Li, L.A. Corkan, J.S. Lindsey, PhotochemCAD: a computer-aided design and research tool in photochemistry, Photochem. Photobiol. 68 (1998) 141–142.
[22] P. Wang, S.M. Zakeeruddin, P. Comte, R. Charvet, R. Humphry-Baker, M. Graetzel, Enhance the performance of dye-sensitized solar cells by co-grafting amphiphilic sensitizer and hexadecylmalonic acid on TiO_2 nanocrystals, J. Phys. Chem. B 107 (2003) 14336–14341.
[23] R. Botros, Azomethine dyes derived from an *o*-hydroxy aromatic aldehyde and a 2-aminopyridine, U.S. Patent 4,051,119 (1977).
[24] D. Guha, A. Mandal, A. Koll, A. Filarowski, S. Mukherjee, Proton transfer reaction of a new orthohydroxy Schiff base in protic solvents at room temperature, Spectrochim. Acta Part A 56 (2000) 2669–2677.
[25] K. Ogawa, J. Harada, T. Fujiwara, S. Yoshida, Thermochromism of salicylideneanilines in solution: aggregation-controlled proton tautomerization, J. Phys. Chem. A 105 (2001) 3425–3427.
[26] A. Koll, A. Filarowski, D. Fitzmaurice, E. Waghorne, A. Mandal, S. Mukherjee, Excited state proton transfer reaction of two new intramolecularly hydrogen bonded Schiff bases at room temperature and 77 K, Spectrochim. Acta Part A 58 (2002) 197–207.
[27] M. Mukhopadhyay, D. Banerjee, A. Koll, A. Filarowski, S. Mukherjee, Proton transfer reaction of a new orthohydroxy Schiff base in some protic and aprotic solvents at room temperature and 77 K, Spectrochim. Acta Part A 62 (2005) 126–131.
[28] H. Dinçalp, F. Toker, İ. Durucasu, N. Avcıbaşı, S. Icli, New thiophene-based azo ligands containing azo methine group in the main chain for the determination of copper(II) ions, Dyes Pigments 75 (2007) 11–24.
[29] H. Joshi, F.S. Kamounah, C. Gooijer, G. van der Zwan, L. Antonov, Excited state intramolecular proton transfer in some tautomeric azo dyes and Schiff bases containing an intramolecular hydrogen, J. Photochem. Photobiol. A: Chem. 152 (2002) 183–191.
[30] J.C. Scaiano, CRC Handbook of Organic Photochemistry, CRC Press Inc., Florida, 1989.
[31] N.J. Turro, Molecular Photochemistry, Benjamin, London, 1965.
[32] P. Suppan, Chemistry and Light, The Royal Society of Chemistry, London, 1994.
[33] L. Moeini-Nombel, S. Matsuzawa, Effect of solvents and a substituent group on photooxidation of fluorene, J. Photochem. Photobiol. A: Chem. 119 (1998) 15–23.
[34] L.M.G. Jansen, I.P. Wilkes, F. Wilkinson, D.R. Worrall, The role of singlet molecular oxygen in the photodegradation of 1-arylazo-2-naphthols in methanol and on cotton, J. Photochem. Photobiol. A: Chem. 125 (1999) 99–106.
[35] J. Pommerehne, H. Vestweber, W. Guss, R.F. Mahrt, H. Bassler, M. Porsch, J. Daub, Efficient 2-layer leds on a polymer blend basis, Adv. Mater. 7 (1995) 551–554.
[36] Y. Belekon, M. Moscalenko, N. Ikonnikov, L. Yashkina, D. Antonov, E. Vorontsov, V. Rozenberg, Asymmetric trimethylsilylcyanation of benzaldehyde catalyzed by (salen)Ti(IV) complexes derived from (R)- and/or (S)-4-hydroxy-5-formyl[2.2]paracyclophane and diamines, Tetrahedron: Asymm. 8 (1997) 3245–3250.
[37] J. Strautch, T.H. Warren, G. Erker, R. Fröhlich, P. Saarenketo, Formation and structural properties of salicylaldiminato complexes of zirconium and titanium, Inorg. Chim. Acta 300–302 (2000) 810–821.
[38] S.J. Coles, M.B. Hursthouse, D.G. Kelly, A.J. Toner, Titanium(IV) complexes of the crystallographically characterised fluorene-Schiff base N-2-fluorenyl(salicylideneimine) and related bi- and tetradentate ligands, Polyhedron 19 (2000) 177–183.
[39] D. Owiny, S. Parkin, F.T. Ladipo, Synthesis, structural determination, and ethylene polymerization chemistry of mono(salicylaldiminato) complexes of titanium(IV), J. Organomet. Chem. 678 (2003) 134–141.
[40] G.P. Pez, N.J. Boonton, Titanium complexes with nitrogen, U.S. Patent 4,024,169 (1977).
[41] A.Z. Abuzuhri, W. Voelter, Applications of adsorptive stripping voltammetry for the trace analysis of metals, pharmaceuticals and biomolecules, Fresenius J. Anal. Chem. 360 (1998) 1–9.
[42] M. Gawrys, J. Golimowski, Novel, sensitive voltammetric methods for titanium determination using chromotropic acid and azo-compounds as complexing agents, Electroanalysis 15 (2003) 1017–1022.
[43] K.R. Millington, K.W. Fincher, A.L. King, Mordant dyes as sensitisers in dye-sensitised solar cells, Sol. Energy Mater. Sol. Cells 91 (2007) 1618–1630.
[44] J. Ohlsson, H. Wolpher, A. Hagfeldt, H. Grennberg, New dyes for solar cells based on nanostructured semiconducting metal oxides: synthesis and characterisation of ruthenium(II) complexes with thiol-substituted ligands, J. Photochem. Photobiol. A: Chem. 148 (2002) 41–48.
[45] D. El Mekkawi, M.S.A. Abdel-Mottaleb, The interaction and photostability of some xanthenes and selected azo sensitizing dyes with TiO_2 nanoparticles, Int. J. Photoenergy 7 (2005) 95–101.